4

SAR Image Formation

4.1 Overview of the Range-Doppler Algorithm

The *range-Doppler algorithm* is a computationally efficient method of focusing raw SAR data into a single look complex (SLC) image (Curlander and McDonough, 1991). The basic SAR theory is conceptually simple (Chapter 2), yet when one looks into the inner workings of the SAR processor, it appears quite complicated. The most difficult part of the problem is related to the coupling between the azimuthal compression and the orbital parameters. In the old days, when the satellite orbits were not known very accurately, one would use techniques such as *clutterlock* and *autofocus* to derive the orbital parameters from the data. This is no longer necessary with the high-accuracy orbits available today. A standard processing sequence follows where the first two steps are done on board the satellite while the remaining four steps are done by the user with a digital SAR processor. The discussion provided here is for the ERS-1 satellite, although the concepts translate to any modern strip-mode SAR satellite. Most of the newer satellite missions (e.g., Sentinel-1, ALOS-2, NISAR) provide SLC images as a basic product, so this focusing step is not needed. Nevertheless, the presentation is helpful for understanding how SLCs are generated.

4.2 Processing Onboard the Satellite

Demodulate The electromagnetic wave consists of a chirp of bandwidth B (~15 MHz) superimposed on carrier frequency ω_o (~5 GHz). To record the return signal, one could simply digitize the amplitude of the electric field $E(t)$ at a sampling rate of 10 GHz using 1-byte encoding. However, this would generate 10 Gbytes of data every second! We are really only interested in how the chirp has been delayed and distorted by the reflection off the Earth's surface. The trick here is to use the shift property of the Fourier transform (Bracewell, 1978, p. 108) to

Downloaded from https://www.cambridge.org/core. UNIVERSIDAD AUTONOMA METROPOLITANA, on 15 Nov 2026 at 10:20:14, subject to the Cambridge Core terms of use, available at https://www.cambridge.org/core/terms. https://doi.org/10.1017/9781009606226.005

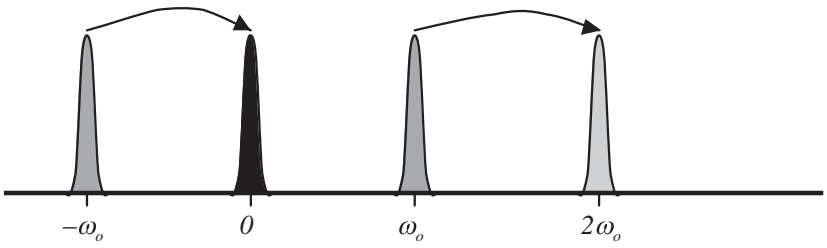


Figure 4.1 Diagram showing the power spectrum of the radar signal before and after shifting by the carrier frequency.

isolate the 15 MHz part of the spectrum containing the chirp. Suppose we multiply the signal $E(t)$ by $e^{i2\pi\omega_o t}$ where ω_o is the carrier frequency. This will shift the Fourier transform of the signal as shown in Figure 4.1.

The function $E(t)$ is a real-valued function, so we know that its Fourier transform has Hermitian symmetry about the origin, that is, $E(-\omega) = E^*(\omega)$. Because of this symmetry, all of the information in the time series is contained within the bandwidth of a single spectral peak. Next, we low-pass filter the signal to isolate the spectral peak centered at the zero frequency. The original signal $E(t)$ was a real-valued function, but after this shift/filter operation, the output is complex. No information is lost in this process and now the output can be digitized at the much lower rate of twice the bandwidth of the chirp (~30 MHz). In the engineering literature, this process is called *heterodyne* and the real and imaginary components are called *in-phase* (I) and *quadrature* (Q).

Digitize The complex signal is digitized at 5 bits per pixel so the numbers range from 0 to 31; the mean value is 15.5. Digitizing the data at 8 bits per pixel would seem more convenient, but transmitting these extra 3 bits to the ground receiving station increases the bandwidth of the telemetry so every effort is made to compress the data before transmission. Once the data are on the ground, they are expanded to 8 bits (one byte) for programming convenience. The raw signal files (e.g., ERS) contain rows of 11 644 bytes that represent a single radar echo (Figure 4.2). The first 412 bytes are timing and other information, while the remaining 11 232 bytes contain the 5 616 complex numbers of raw signal data.

4.3 Digital SAR Processing

The digital SAR processor is a computer program (*esarp* in GMTSAR) that converts the raw signal data (***.raw**) into a SLC image (***.SLC**). An overview is provided in Figure 4.3, followed by a detailed description of each step. The parameter file (***.PRM**, Table 4.1) contains all the parameters needed to focus the image.

Downloaded from https://www.cambridge.org/core. UNIVERSIDAD AUTONOMA METROPOLITANA, on 15 Nov 2026 at 10:20:14, subject to the Cambridge Core terms of use, available at https://www.cambridge.org/core/terms. https://doi.org/10.1017/9781009606226.005

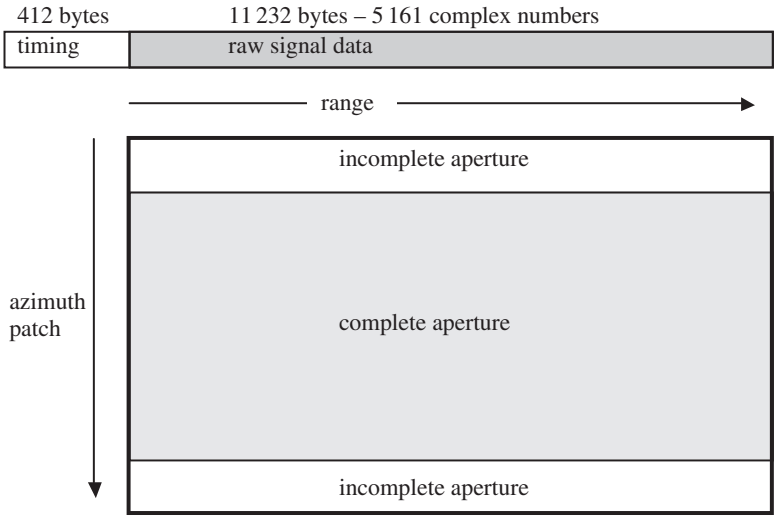


Figure 4.2 Raw signal data.

1. *Range compression* A sharp radar pulse is recovered by deconvolution of the chirp. This is done with fast Fourier transform (FFT). There are 5 616 points in the ERS-1 signal data and the chirp is 703 points long. Both are zero-padded to a length of 8 192 prior to deconvolution to take advantage of the speed of the radix-2 FFT algorithms. Later, we keep 6 144 points, which enables one to extract the phase beyond the edges of the original swath. Since the chirp really did interact with the ground outside the digitized swath, this is not magic. The number 6 144 has small prime factors that may be optimal for later 2-D FFT phase unwrapping algorithms.
2. *Patch processing* The next step is to focus the image in the along-track or azimuth direction. This is also done by FFT, but now we need to process columns rather than rows. For the ERS radar, the synthetic aperture is 1 296 points long so we need to read at least that many rows into the memory of the computer. Actually, 4 096 rows is a better number since it is a power of 2. A typical ERS raw data file has 28 000 rows so we will need to process many of these *patches*. One problem with this approach is that the synthetic aperture is only complete for the inner 2 800 points of the 4 096 data patch so the patches must have a 1 296-point overlap (Figure 4.2). A $4\,096 \times 5\,616$ patch requires at least 184 Mbytes of computer memory for single precision real numbers. In the old days, before this large memory space was available, each patch was transposed–*corner turning*–using high-speed disks so the data could be processed on a column-by-column basis. The L-band data from ALOS have

Downloaded from https://www.cambridge.org/core. UNIVERSIDAD AUTONOMA METROPOLITANA, on 15 Nov 2026 at 10:20:14, subject to the Cambridge Core terms of use, available at https://www.cambridge.org/core/terms. https://doi.org/10.1017/9781009606226.005

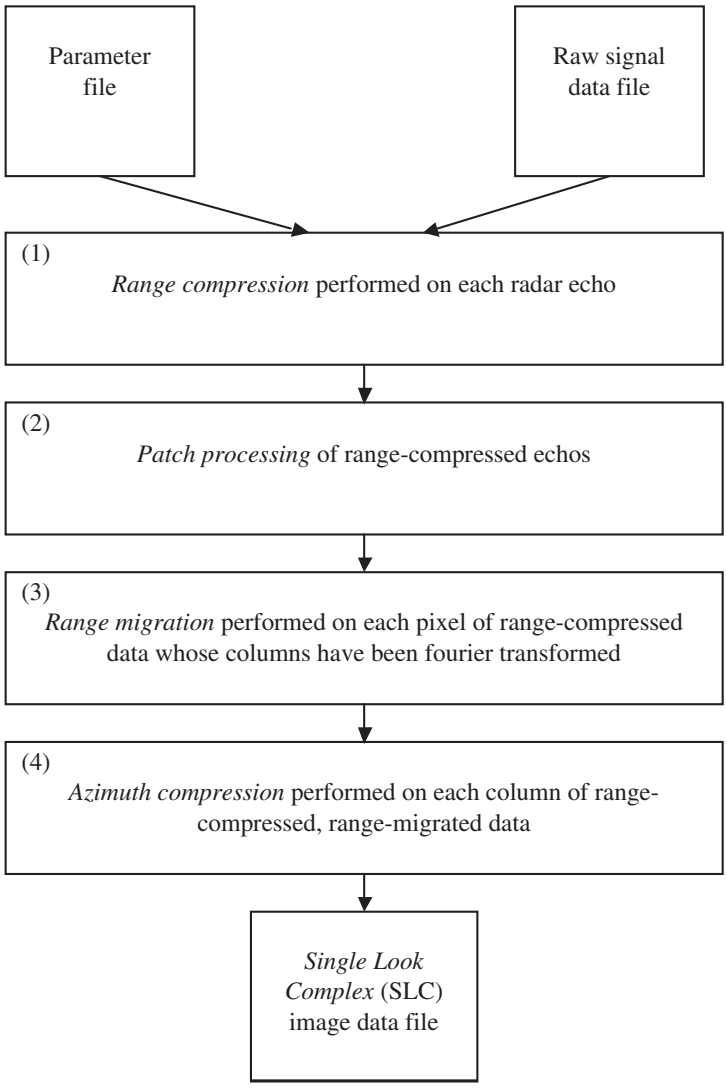


Figure 4.3 Digital SAR processing overview.

a much longer synthetic aperture and patch size. Efficient processing of these data requires a minimum of 2 Gbytes of computer memory.

3. *Range migration* As we will see later, a point target will appear as a hyperbolic-shaped reflection as it moves through the synthetic aperture. In addition, there could be a pronounced linear drift due to an elliptical orbit and Earth's rotation. In other words, the target will migrate in the range cell as a linear trend plus a hyperbola. The shape of this migration path is calculated from the precise orbital information and is approximated by a parabola. Prior to focusing the

Downloaded from https://www.cambridge.org/core. UNIVERSIDAD AUTONOMA METROPOLITANA, on 15 Nov 2026 at 10:20:14, subject to the Cambridge Core terms of use, available at https://www.cambridge.org/core/terms. https://doi.org/10.1017/9781009606226.005

Table 4.1 *Example parameter (PRM) file (e2_10001_2925.PRM).*

File information/format			
input_file	e2_10001_2925.raw	name of raw data file	
SC_identity	2	(1) – ERS-1 or (2) – ERS-2	
bytes_per_line	11 644	number of bytes in row of raw data	
first_sample	206	412 bytes of timing information to skip over	
fd1	248.115	Doppler centroid estimated from data	f_{Dc}
I_mean	15.5	mean value of real numbers	
Q_mean	15.5	mean value of imaginary numbers	
icu_start	2576039268.848	spacecraft clock for first sample	
SC_clock_start	1997078.767881851	UTC for first sample YYYDDD.DDDDDDDD	
SC_clock_stop	1997078.768074699	UTC for last sample YYYDDD.DDDDDDDD	
Radar characteristics			
PRF	1679.902394	pulse repitition frequency	PRF
rng_samp_rate	1.89625e+07	range sampling rate	f_s
chirp_slope	4.17788e+11	chirp slope	k
pulse_dur	3.712e-05	pulse duration	τ_p
radar_wavelength	0.056666	radar wavelength	λ
Orbital information			
near_range	829924.365777	distance to first range bin	R_{near}
earth_radius	6371746.4379	earth radius 1/2 way into image	R_e
SC_height	787955.52	spacecraft height above the earth_radius	H
SC_vel	7125.0330	effective speed	V_e
Processing information			
num_valid_az	2 800	size of patch to process	
num_patches	10	number of patches to process	
first_line	1		
deskew	n	deskew (yes or no)	
st_rng_bin	1	start processing at row number	
num_rng_bins	6 144	number of range bins in output file	
chirp_ext	614	extend the chirp to process outside swath	
Flip_iq	n	exchange real and imaginary numbers (yes or no)	
nlooks	1	number of azimuth echoes to average	
Image alignment			
rshift	15.1	range shift to align image to master	
ashift	483.2	azimuth shift to align image to master	
stretch_r	0.0014569	range stretch versus range	
stretch_a	−0.0019436	azimuth stretch versus range	
a_stretch_r	0	range stretch versus azimuth	
a_stretch_a	0	azimuth stretch versus azimuth	

Downloaded from https://www.cambridge.org/core. UNIVERSIDAD AUTONOMA METROPOLITANA, on 15 Nov 2026 at 10:20:14, subject to the Cambridge Core terms of use, available at https://www.cambridge.org/core/terms. https://doi.org/10.1017/9781009606226.005

image along a single column, these signals must be migrated back to a constant range cell. This is called *range migration* and the fastest way to do this is by Fourier transforming the columns first. Each Fourier component corresponds to a unique Doppler shift and also a unique value of range migration; for an ideal radar, the first component will have zero Doppler and will correspond to the point on the Earth that is perpendicular to the spacecraft velocity vector. The second component will have a small positive Doppler shift and a small migration of the range cells will be needed – and so on all the way through the positive and negative Doppler spectrum.

4. *Azimuth compression* The final step in the processing is to focus the data in azimuth by accounting for the phase shift of the target as it moves through the aperture. In Chapter 2, we calculated the illumination pattern on a screen due to the propagation of a coherent wave from the aperture to the screen. The azimuth compression relies on the same theory, although we do the opposite calculation–given the illumination pattern, calculate the shape of the aperture (reflectivity of the target). This is done by generating a second frequency-modulated chirp where the chirp parameters depend on the velocity of the spacecraft, the pulse repetition frequency (PRF), and the absolute range. The chirp is Fourier transformed into Doppler space and multiplied by each column of range-migrated data. The product is inverse Fourier transformed to provide the focused image.

   Single-Look Complex image As described earlier, only the inner 2 800 rows use the complete synthetic aperture so these are written to an output file (Figure 4.2). The file-reading pointer is moved back 1 296 rows to start the processing of the next patch. Because complete apertures are used for each patch, they will abut seamlessly.

4.4 Range Compression

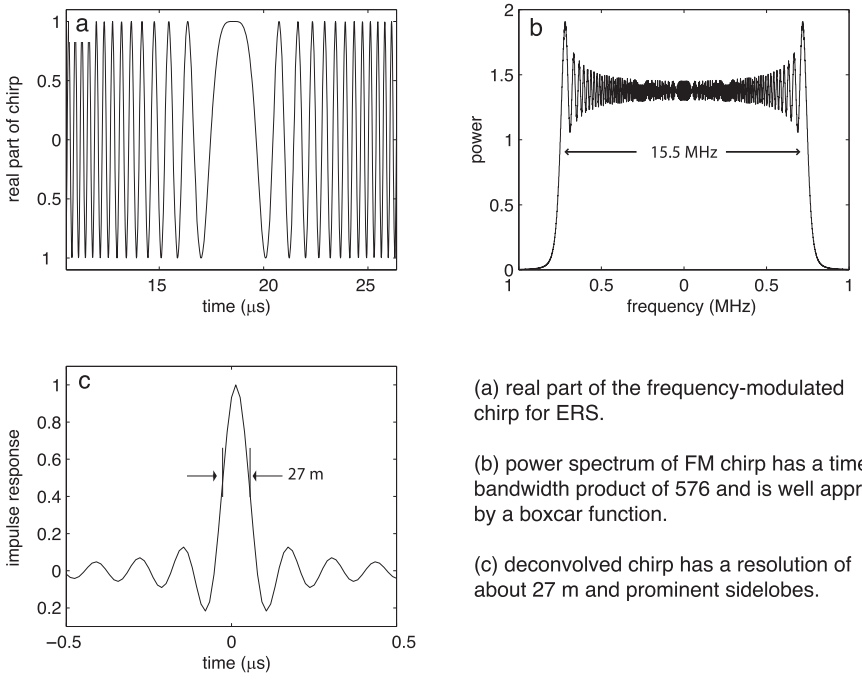
To reduce the peak power of the radar transmitter associated with a short pulse, a long FM chirp is emitted by the radar. This chirp propagates to the ground where it reflects from a swath typically 85 km wide. When it returns to the radar, the raw signal data consists of the complex reflectivity of the surface convolved with the chirp. Our objective is to recover the complex reflectivity by deconvolution of the chirp. As discussed earlier, this is the first step in the digital SAR processor. For the ERS radar, the frequency-modulated chirp is

$$S(t) = e^{i\pi k t^2} \qquad |t| < \tau_p/2. \tag{4.1}$$

where

k chirp slope ($4.17788 \times 10^{11} s^{-2}$)

Downloaded from https://www.cambridge.org/core. UNIVERSIDAD AUTONOMA METROPOLITANA, on 15 Nov 2026 at 10:20:14, subject to the Cambridge Core terms of use, available at https://www.cambridge.org/core/terms. https://doi.org/10.1017/9781009606226.005



(a) real part of the frequency-modulated chirp for ERS.

(b) power spectrum of FM chirp has a time-bandwidth product of 576 and is well approximated by a boxcar function.

(c) deconvolved chirp has a resolution of about 27 m and prominent sidelobes.

Figure 4.4 Chirp for ERS-1.

τ_p pulse duration ($3.712 \times 10^{-5} s$ or ~11 km long)
f_s range sampling rate ($1.89625 \times 10^7 s^{-1}$).

An example of a portion of the chirp for the ERS radar as well as its power spectrum and impulse response is shown in Figure 4.4.

The bandwidth of the chirp, $B = k\tau_p$, has a value of 15.5 MHz for the ERS radar. A matched filter is used to deconvolve the chirp from the data. In this case, the matched filter is simply the complex conjugate of the chirp or $S^*(t) = e^{-i\pi kt^2}$. The convolution of $S^*(t)$ and $S(t)$ is shown in Figure 4.4 (c). The effective range resolution of the radar is about 27 m.

Using computer code and the radar parameters provided in the PRM file, one can deconvolve the ERS chirp. Figure 4.5 is a small patch of ERS-2 data for an area around Piñon Flat, California (track 127, frame 2 925, orbit 10 001). This area contains two radar reflectors (Figure 4.5 and Table 4.2) spaced about 600 m apart that were installed in late 1996. The amplitude of the raw signal data appears as noise with a single horizontal streak due to missing data (Figure 4.5 (a)). The range-compressed data (right image) shows two vertical streaks due to the high reflectivity of the reflectors (red circles) as they migrate through the synthetic aperture.

Downloaded from https://www.cambridge.org/core. UNIVERSIDAD AUTONOMA METROPOLITANA, on 15 Nov 2026 at 10:20:14, subject to the Cambridge Core terms of use, available at https://www.cambridge.org/core/terms. https://doi.org/10.1017/9781009606226.005

Table 4.2 *Coordinates of Radar Reflectors.*

position			orientation	
lat.	*lon.*	*height*	*elev.*	*azi.*
33.612246	−116.456768	1258.990	39°	257.5°
33.612246	−116.457893	1257.544	39°	102.5°
33.607373	−116.451836	1254.537	39°	102.5°

Latitude and longitude in decimal degrees and height in meters relative to the WGS-84 coordinate system and ellipsoid. The survey point is the apex (lowest corner) of each reflector. There should be a correction for the offset between the phase center of the reflector and the apex.

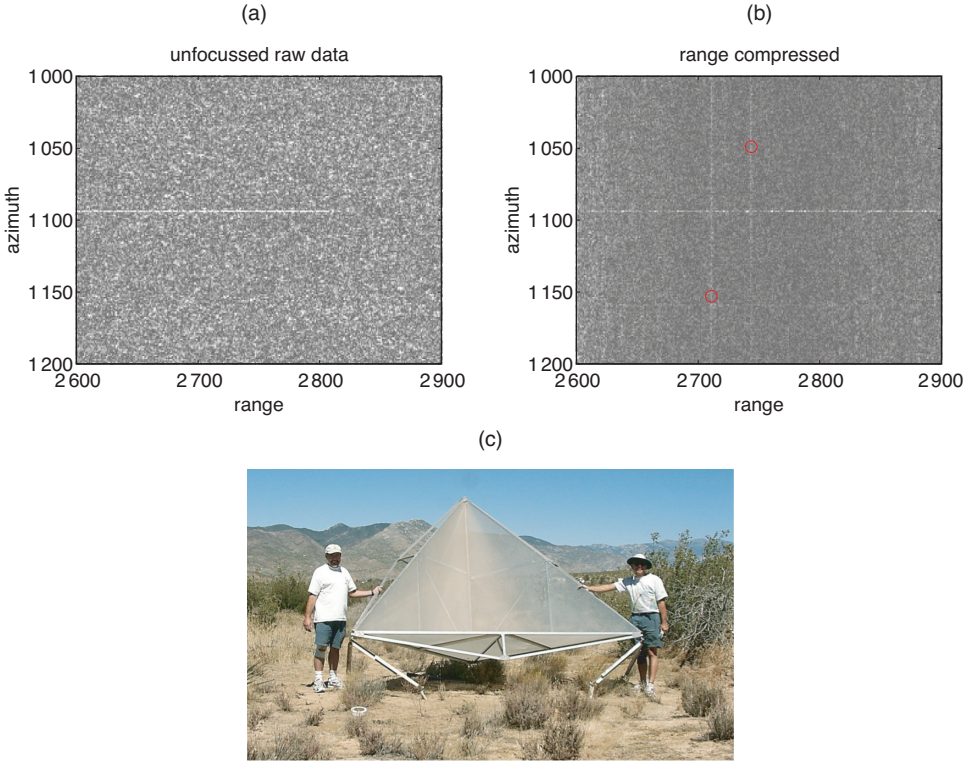


Figure 4.5 Raw ERS signal data (a) and range-compressed data (b) for data over Piñon Flat California where three radar corner reflectors are installed (c).

4.5 Azimuth Compression

Azimuth compression or azimuth focusing involves coherent summation of echos at a constant range from the point reflector. The geometry of the strip-mode

Downloaded from https://www.cambridge.org/core. UNIVERSIDAD AUTONOMA METROPOLITANA, on 15 Nov 2026 at 10:20:14, subject to the Cambridge Core terms of use, available at https://www.cambridge.org/core/terms. https://doi.org/10.1017/9781009606226.005

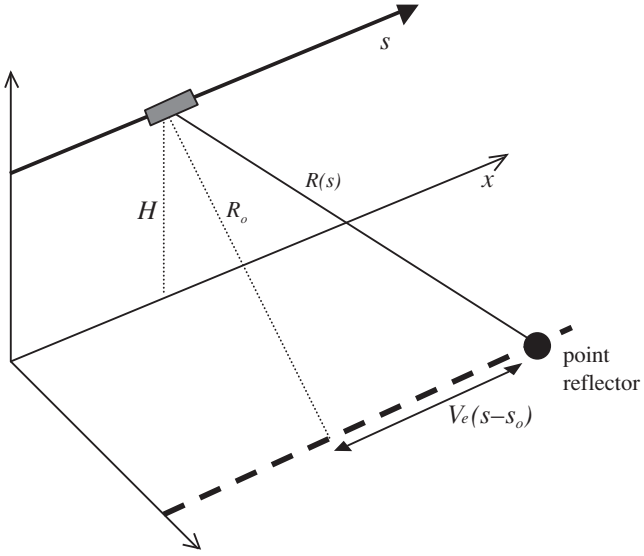


Figure 4.6 Geometry of radar passing over a point reflector where:

V_e	the effective speed as discussed later
s	slow time along the satellite track
s_o	time when the center of the radar echo passes over the point reflector
R_o	$R_{near} + n * (c/f_s)$ minimum range from the spacecraft to the target
R_{near}	near range to first data sample in the swath

acquisition is shown in Figure 4.6. The range to the point reflector evolves with time as

$$R^2(s) = R_o^2 + V_e^2(s - s_o)^2. \tag{4.2}$$

The complex phase of the return echo is

$$C(s) = \exp\left[-i\,\frac{4\pi}{\lambda}R(s)\right]. \tag{4.3}$$

The range versus slow time is approximately a hyperbola but for mathematical convenience we'll approximate this using a parabola

$$R(s) = R_o + \dot{R}(s - s_o) + \frac{\ddot{R}}{2}(s - s_o)^2 + \cdots \tag{4.4}$$

where the dot indicates derivative with respect to slow time, s. Curlander and McDonough (1991) discuss the accuracy of this polynomial approximation and it is also discussed later in terms of the ALOS SAR. The approximation is good enough for strip-mode SAR but may be inadequate for the much longer apertures associated with spotlight-mode SAR. Now we can write the phase of the return

Downloaded from https://www.cambridge.org/core. UNIVERSIDAD AUTONOMA METROPOLITANA, on 15 Nov 2026 at 10:20:14, subject to the Cambridge Core terms of use, available at https://www.cambridge.org/core/terms. https://doi.org/10.1017/9781009606226.005

signal as a function range, range rate, and range acceleration.

$$C(s) = \exp\left\{-i\,\frac{4\pi}{\lambda}\left[R_o + \dot{R}\,(s - s_o) + \ddot{R}(s - s_o)^2/2\right]\right\}. \tag{4.5}$$

It is more common to describe the parameters for focusing the SAR image as the Doppler centroid f_{Dc} and the Doppler frequency rate f_R. The relationships are:

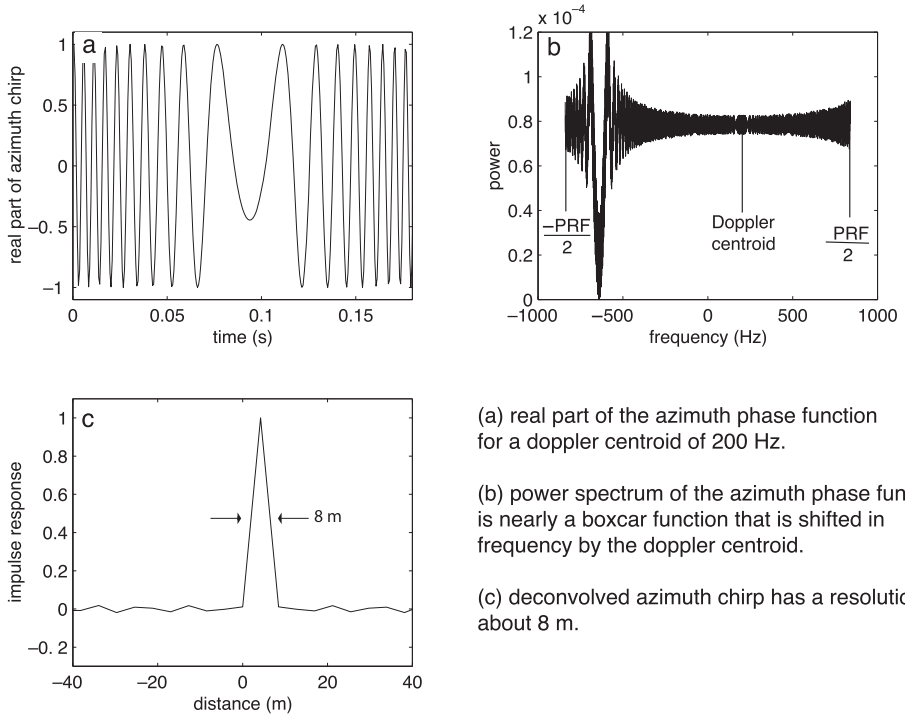
$$f_{Dc} = \frac{-2\dot{R}}{\lambda} \quad \text{and} \quad f_R = \frac{-2\ddot{R}}{\lambda} \tag{4.6}$$

or

$$C(s) = \exp\left\{-i\,\frac{4\pi R_o}{\lambda}\right\}\,\exp\left\{i2\pi\left[f_{Dc}\,(s - s_o) + f_R(s - s_o)^2/2\right]\right\}. \tag{4.7}$$

Note that this function is another frequency-modulated chirp where the parameters are the Doppler centroid and the Doppler frequency rate. An example of this azimuthal chirp function for the ERS orbit/radar as well as its power spectrum and impulse response are shown in Figure 4.7.

The bandwidth of the azimuthal chirp is equal to the PRF (PRF = 1 680 Hz). In this case the matched filter is simply the complex conjugate of the azimuthal phase function (Equation 4.7) or $C^*(s)$.



(a) real part of the azimuth phase function for a doppler centroid of 200 Hz.

(b) power spectrum of the azimuth phase function is nearly a boxcar function that is shifted in frequency by the doppler centroid.

(c) deconvolved azimuth chirp has a resolution of about 8 m.

Figure 4.7 Azimuthal phase for the ERS-1 spacecraft.

Downloaded from https://www.cambridge.org/core. UNIVERSIDAD AUTONOMA METROPOLITANA, on 15 Nov 2026 at 10:20:14, subject to the Cambridge Core terms of use, available at https://www.cambridge.org/core/terms. https://doi.org/10.1017/9781009606226.005

Doppler centroid, Doppler rate, and effective speed Proper focus of the image requires accurate estimates of the three parameters given in Equations 4.5 and 4.7. Actually, we only need to estimate two parameters because we will sweep through the range cells n in the raw data file and focus the image at each range $R_o = R_{near} + n^*(C/f_s)$ where C is the speed of light and f_s is the range sampling rate. Ideally, the beam of the radar would be steered so that it is centered at a point on the ground where the range is minimum so the Doppler centroid is zero or at least small. We follow the approach of Madsen (1989) and calculate the Doppler centroid directly from the raw data file by computing the average change in phase between adjacent rows of the raw data file. This assumes that the Doppler centroid does not vary with slow time, although it could vary slightly with increasing range. We use this estimated Doppler centroid to focus the image (or select a similar Doppler centroid that is closest to the mean of a stack of repeated SAR images).

Finally, as discussed later, the precise orbit (i.e., in Earth-fixed coordinates) can be used to calculate the third parameter, the range acceleration $\ddot{R}$. One approach would be to use the precise orbit to calculate range acceleration for each range, but this is unnecessary because there is a good formula for range acceleration as a function of range that involves a parameter called the effective speed V_e of the spacecraft. Indeed, the SAR processor code takes effective speed and converts this to $\ddot{R}$ to focus the image. The derivation of the effective speed parameter follows. We start by taking the first derivative of the range squared versus slow time given in Equation 4.2.

$$\frac{\partial R^2\,(s)}{\partial s} = 2R\dot{R} = 2V_e^2 s. \tag{4.8}$$

The second derivative is

$$\dot{R}\dot{R} + R\ddot{R} = V_e^2. \tag{4.9}$$

Next we assume that the radar antenna is oriented nearly perpendicular to the velocity vector of the satellite so $\dot{R} << V_e$. Note that to achieve interferometric coherence, the radar beams of the reference and repeat images must overlap spatially, which essentially requires that the Doppler centroid be less than half of the PRF. Given a typical PRF for a spaceborne SAR of 2 000 Hz and using Equation 4.6 and a wavelength of 0.05 m, the range rate must be less than 25 m/s. This is much less than the typical spacecraft velocity of 7 800 m/s so we can safely ignore the first term on the left-hand side of Equation 4.9. So the approach is to use the precise orbit to calculate the range acceleration $\ddot{R}$ at a single range R_o within the image. These two numbers are used to calculate the effective speed

Downloaded from https://www.cambridge.org/core. UNIVERSIDAD AUTONOMA METROPOLITANA, on 15 Nov 2026 at 10:20:14, subject to the Cambridge Core terms of use, available at https://www.cambridge.org/core/terms. https://doi.org/10.1017/9781009606226.005

$$V_e = \sqrt{R_o \ddot{R}}. \tag{4.10}$$

Finally, this parameter is used by the SAR processing code to calculate the range acceleration

$$\ddot{R} = V_e^2 / R \tag{4.11}$$

at all the other ranges in the swath.

The effective speed, which is reported as SC_vel in the PRM file, can be used to compute the ground track speed V_g of the satellite as

$$V_g = \frac{V_e}{\left(1 + \frac{H}{R_e}\right)^{1/2}}. \tag{4.12}$$

where H is the height of the spacacraft and R_e is the local Earth radius. Also note that $V_g < V_e < V_s$ where V_s is the velocity of the spacecraft at orbital altitude. Using Equation 4.12, one can show that

$$V_e = \frac{V_s}{\left(1 + \frac{H}{R_e}\right)^{1/2}}. \tag{4.13}$$

Note this is only an approximate formula for computing the effective speed from the spacecraft velocity (Curlander and McDonough (1991)). For C-band radars such as ERS and Envisat, the effective speed calculated from Equation 4.13 provides adequate focus for the SAR image. However, for L-band SARs such as ALOS, the aperture is much longer, so other factors must be considered such as the curvature and ellipticity of the orbit.

We bypass this complexity by computing the effective speed from a polynomial fit of range versus time as discussed later, but first we discuss the length of the synthetic aperture.

Length of synthetic aperture The length of the synthetic aperture L_a depends on the length of the radar ground footprint in the azimuth direction, which is approximately

$$L_a = R_o \frac{\lambda}{L} \tag{4.14}$$

where L is the physical length of the antenna, λ is the wavelength and R_o is the slant range given earlier. The length of the aperture in terms of radar echoes is given by

$$n_a = \frac{L_a \mathrm{PRF}}{V_e}. \tag{4.15}$$

This is simply the length of the synthetic aperture divided by the along-track sampling distance. Table 4.3 provides these quantities for SARs of interest for interferometry today.

Downloaded from https://www.cambridge.org/core. UNIVERSIDAD AUTONOMA METROPOLITANA, on 15 Nov 2026 at 10:20:14, subject to the Cambridge Core terms of use, available at https://www.cambridge.org/core/terms. https://doi.org/10.1017/9781009606226.005

Table 4.3 *Length of synthetic aperture for three satellites.*

	V_e (m/s)	λ (m)	PRF (Hz)	R_o (km)	L (m)	L_A (m)	n_a *theory*	n_a *actual*
ERS-1/2	7 125	0.057	1 679	~850	10	4 850	1 142	1 164
Envisat	7 125	0.057	2 067	~1 020	10	5 830	1 690	1 740
ALOS	7 125	0.236	2 159	~1 020	9	26 830	8 128	9 216

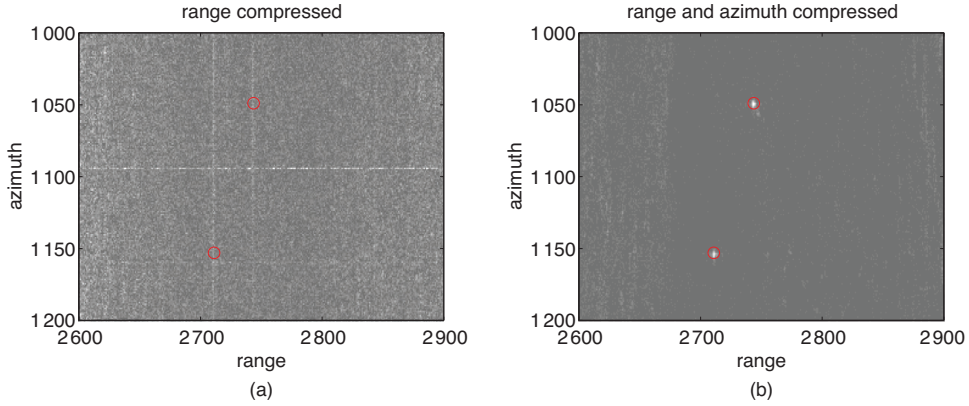


Figure 4.8 Range-compressed (a) and fully focused image (b). The two bright reflectors are 3-m corner cubes at Piñon Flat observatory. These were deployed in 1996 and therefore provide stable calibration points for ERS-1, ERS-2, Envisat, ALOS, and all future satellites.

Focused image Using the azimuth compression formulas and parameters provided earlier, one can focus the image in the azimuth direction. Figure 4.8 show the same small patch of ERS-2 data for an area of Piñon Flat, California. The range-compressed data (Figure 4.8 (a)) shows two vertical streaks due to the high reflectivity of the reflectors (red circles) as they migrate through the synthetic aperture. The fully focused image (Figure 4.8 (b)) shows the point-like reflectivity associated with the two radar reflectors.

4.5.1 Estimating $\ddot{R}$ when a Precise Orbit Is Available

(This subsection can be skipped unless the reader wants to understand the geometric details for computing $\ddot{R}$ from the precise orbit.) Estimation of the range acceleration from the orbit seems conceptually simple, although there is one complication that requires a bit of geometry. The complication is to find a point on the surface of the Earth, at a prescribed range, and convert that location to Cartesian coordinates. Consider the following three vectors that form a triangle:

Downloaded from https://www.cambridge.org/core. UNIVERSIDAD AUTONOMA METROPOLITANA, on 15 Nov 2026 at 10:20:14, subject to the Cambridge Core terms of use, available at https://www.cambridge.org/core/terms. https://doi.org/10.1017/9781009606226.005

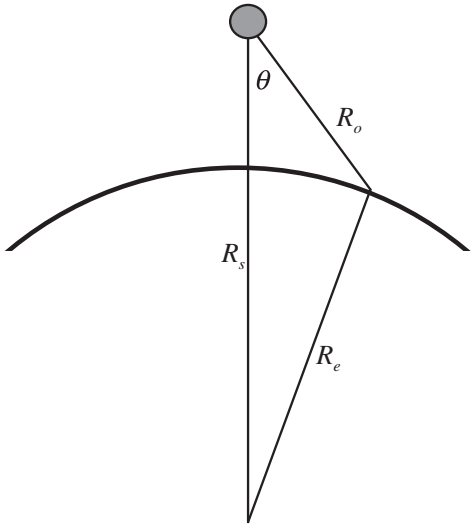


Figure 4.9 Triangle of Earth radius, satellite radius, and range to a point on the surface of the Earth used to compute look angle θ.

$\vec{R}_s$ the vector position of the satellite in the Earth-fixed coordinate system;
$\vec{R}_e$ the vector position of a point scatterer on the Earth and somewhere in the SAR scene;
$\vec{R}_o$ the line-of-sight (LOS) vector between the satellite and the point scatterer.

The three vectors form a triangle such that $\vec{R}_e = \vec{R}_s + \vec{R}_o$ (Figure 4.9). The scalar range, which is a function of slow time, is given by

$$R(s) = \left|\vec{R}_s(s) - \vec{R}_e\right| \cong R_o + \dot{R}_o(s - s_o) + \frac{\ddot{R}_o}{2}(s - s_o)^2 + \ldots \tag{4.16}$$

Measurements of scalar range versus slow time can be used to estimate the coefficients of the parabolic approximation. The algorithm is to:

1. Use the precise orbit to calculate the position vector of the satellite and compute a time series $R(s)$ over the length of the aperture.
2. Perform a least-squares parabolic fit to this time series to estimate R_o, $\dot{R}_o$, $\ddot{R}_o$.
3. Compute the effective speed as $V_e^2 = R_o\ddot{R}_o$.

The only remaining step is to calculate the position of the point target $\vec{R}_e = \vec{R}_s + \vec{R}_o$. Actually this can be any point in the image so the selection criteria is that the point lie at the proper radius of the surface of the Earth $R_e = \left|\vec{R}_e\right|$ and the $\vec{R}_o$ vector is perpendicular to the velocity vector of the satellite $\vec{V}$. If we prescribe the length of the R_o- vector, then the angle between the satellite position vector and the LOS vector is given by the law of cosines as shown in Figure 4.9.

Downloaded from https://www.cambridge.org/core. UNIVERSIDAD AUTONOMA METROPOLITANA, on 15 Nov 2026 at 10:20:14, subject to the Cambridge Core terms of use, available at https://www.cambridge.org/core/terms. https://doi.org/10.1017/9781009606226.005

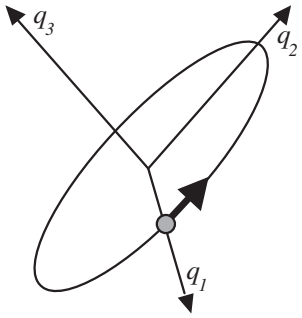


Figure 4.10 Satellite (gray) in circular inclined orbit about the Earth.

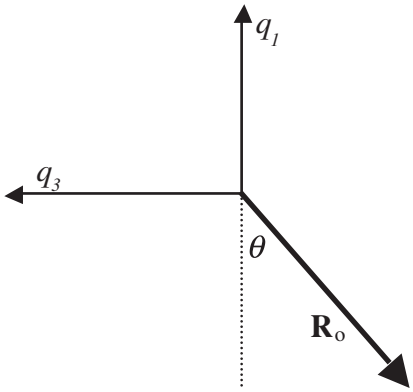


Figure 4.11 Diagram of satellite-fixed coordinate system where q_1 is the vector from the center of the Earth to the spacecraft, and q_2 is parallel to the velocity vector of the SC. The bold vector is the look vector of the radar where θ is the look angle.

This diagram has the satellite at the gray dot with the velocity vector pointing into the page. The cosine of the look angle is

$$\cos\theta = \frac{\left(R_s^2 + R_o^2 - R_e^2\right)}{2R_sR_o}. \tag{4.17}$$

Next consider a local coordinate system where the q_2 axis is aligned with the velocity vector of the satellite as shown in Figure 4.10.

In this coordinate system, the q_1 axis is parallel to $\vec{R}_s$, the q_2 axis is parallel to $\vec{V}$, and the q_3 axis is perpendicular to both and is given by their cross product

$$q_3 = \frac{\vec{R}_s}{|R_s|} \times \frac{\vec{V}}{\left|\vec{V}\right|}. \tag{4.18}$$

Downloaded from https://www.cambridge.org/core. UNIVERSIDAD AUTONOMA METROPOLITANA, on 15 Nov 2026 at 10:20:14, subject to the Cambridge Core terms of use, available at https://www.cambridge.org/core/terms. https://doi.org/10.1017/9781009606226.005

Figure 4.11 has the velocity vector of the satellite going into the page and aligned with the q_2 coordinate. The q_1 vector is the radial vector from the center of the Earth. The LOS right-look vector is in the q_1-q_3 plane as shown in Figure 4.11. After going through this geometry, we find the LOS vector to a point on the surface of the Earth at the prescribed range for a right-looking radar is

$$\vec{R}_o = R_o \left(-\cos\theta \hat{q}_1 \quad 0\hat{q}_2 \quad -\sin\theta \hat{q}_3 \right) \tag{4.19}$$

and for a left-looking radar is

$$\vec{R}_o = R_o \left(-\cos\theta \hat{q}_1 \quad 0\hat{q}_2 \quad \sin\theta \hat{q}_3 \right). \tag{4.20}$$

4.6 Example with ALOS L-Band Orbit

Now that we have an algorithm for finding a point on the surface of the Earth that is within the SAR scene, we can compute the time evolution of the range to that point as the satellite orbits above the rotating Earth. We consider data from a descending orbit over Koga, Japan, where three radar reflectors have been deployed. The image is a fine beam, single polarization having a nominal look angle of 34.3 degrees. A Hermite polynomial interpolation was used to calculate the $x - y - z$ position of the satellite from 28 position and velocity vectors spaced at 60-second intervals. Thus, the entire arc is 28 minutes or a quarter of an orbit. The accuracy of the Hermite interpolator was checked by omitting a central point and performing an interpolation using 6 surrounding points. The accuracy of the interpolation was found to be better than 0.2 mm suggesting that the 60-s interval provides an accurate representation of the orbital arc.

Next we compute the range to the ground point as a function of time before and after the perpendicular LOS vector $\vec{R}_o$. We used a before/after time interval of 3 seconds, which is about 1.5 times the length of the synthetic aperture for ALOS. A second-order polynomial was fit to the range versus time function and the three coefficients provide estimates of R_o, $\dot{R}_o$, and $\ddot{R}_o$. The range versus time, as well as the residual of the fit, are shown in Figure 4.12. One can learn a great deal from this exercise.

1. The first thing learned is that the parabolic approximation to a hyperbola used in the SAR processor has a maximum error of about 1 cm at a time offset of 3 seconds. This corresponds to a small fraction of the 23-cm wavelength. Note that the actual aperture length for ALOS is only ±2 seconds so this approximation is justified.
2. The range at zero offset has an error of −0.24 m. This is due to approximating the shape of the Earth as a sphere having a local radius given by the WGS84 ellipsoid formula. In other words, there is a small error in the LOS vector

Downloaded from https://www.cambridge.org/core. UNIVERSIDAD AUTONOMA METROPOLITANA, on 15 Nov 2026 at 10:20:14, subject to the Cambridge Core terms of use, available at https://www.cambridge.org/core/terms. https://doi.org/10.1017/9781009606226.005

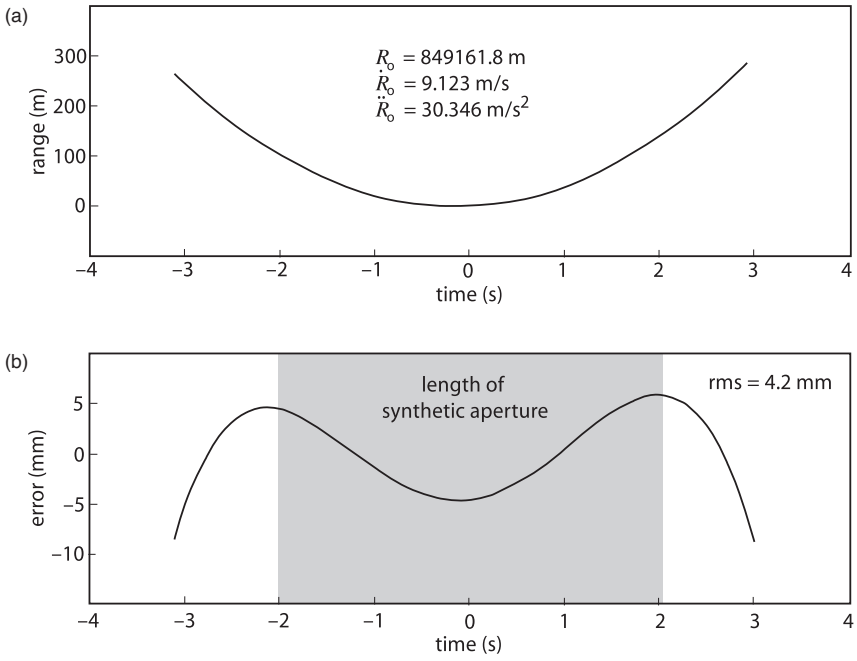


Figure 4.12 (a) range versus slow time for ALOS for a 6-second aperture. The actual aperture is 4.2 seconds (Table 4.3). (b) deviation from a parabolic fit to this range vs. time function. The shaded area is the length of the synthetic aperture.

because it intersects the surface of the Earth at a latitude that is slightly different from the spacecraft latitude so the Earth radii will differ slightly.

3. The Doppler shift when the satellite is perpendicular to the target can be calculated from the range rate coefficient using Equation 4.6.
4. Finally, the range acceleration can be used to calculate the effective speed of the satellite $V_e^2 = R_o\ddot{R}_o$. For this example we arrive at a speed of 7 174 m/s. By trial and error we found the optimal focus parameter corresponds to a speed between 7 173 and 7 183 m/s, so this new estimate is accurate. The simple spherical orbit ground speed approximation (4.13) yields an estimate of 7 208 m/s which provides poor focus.

Squint angle – Finally let's examine the quantity, $\frac{V(s-s_o)}{R_o}$. This is related to something called the squint angle, γ, as shown in Figure 4.13.

The squint angle is simply

$$\gamma = \tan^{-1}\left(\frac{V(s-s_o)}{R_o}\right). \tag{4.21}$$

For the ERS, Envisat, and ALOS satellites, the squint angle is adjusted so the zero Doppler occurs roughly in the center of the antenna beam pattern. If the satellite

Downloaded from https://www.cambridge.org/core. UNIVERSIDAD AUTONOMA METROPOLITANA, on 15 Nov 2026 at 10:20:14, subject to the Cambridge Core terms of use, available at https://www.cambridge.org/core/terms. https://doi.org/10.1017/9781009606226.005

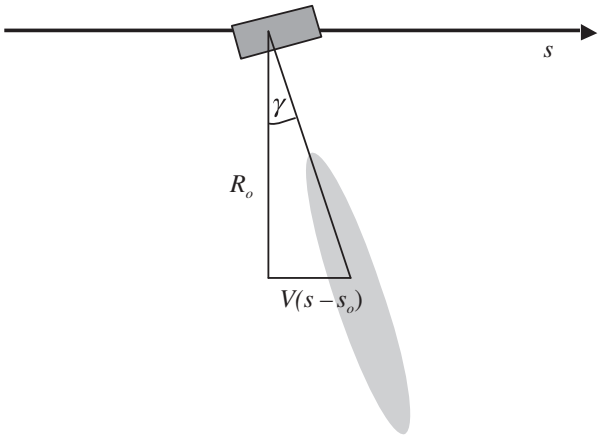


Figure 4.13 Schematic diagram of squint angle.

orbit was circular and the Earth was a nonrotating sphere, then the zero Doppler would correspond to a zero squint angle.

For interferometry it is important that the beam patterns of the reference and repeat orbits have a large overlap (>50%) at a given along-track spacecraft position. The requirement is that the Doppler centroid of the reference and repeat passes agree to about 1/2 of the PRF. In late 1999, the gyroscopes on ERS-2 failed, so it became difficult to control the squint angle of the spacecraft. Data acquired after this date may have a Doppler centroid outside of the acceptable range and thus may be useless for interferometry. The squint angle for the ALOS satellite is well controlled and the Doppler centroid is usually less than 100 Hz so we commonly focus the images at zero Doppler.

4.7 Problems

1. Explain why the raw signal data are provided as complex numbers. Why are the numbers restricted to the range 0–31?
2. Why is the SAR processing with the range-Doppler algorithm often done in patches rather than all at once? What is the minimum possible patch size?
3. Most SAR instruments emit a frequency-modulated chirp rather than a short pulse. Why? Write a Matlab program to deconvolve the FM chirp for ERS and reproduce the impulse response function shown in Figure 4.4.
4. Make a plot of the real and imaginary parts of the function given in Equation 4.5 for a time interval of −0.1 to 0.1 seconds. Use $R_o = 850$ km, $\dot{R}_o = 0$, $\ddot{R}_o = \frac{V^2}{R_o}$, where $V = 7\,125 \text{ms}^{-1}$. Use a wavelength of 56 mm.
5. Derive Equation 4.13.

Downloaded from https://www.cambridge.org/core. UNIVERSIDAD AUTONOMA METROPOLITANA, on 15 Nov 2026 at 10:20:14, subject to the Cambridge Core terms of use, available at https://www.cambridge.org/core/terms. https://doi.org/10.1017/9781009606226.005

6. Derive Equation 4.14. (You may need to look back at Chapter 2.)
7. Explain qualitatively how a SAR antenna should be squinted (turned) to keep the Doppler centroid of the return echoes close to zero for the following three cases: (1) an elliptical orbit about a spherical, nonrotating Earth; (2) a circular orbit about an elliptical and nonrotating Earth; (3) and a circular orbit about a rotating, spherical Earth.

Downloaded from https://www.cambridge.org/core. UNIVERSIDAD AUTONOMA METROPOLITANA, on 15 Nov 2026 at 10:20:14, subject to the Cambridge Core terms of use, available at https://www.cambridge.org/core/terms. https://doi.org/10.1017/9781009606226.005